Essential Readings in Light Metals: Electrode Technology for Aluminum Production.
Edited by Alan Tomsett and John Johnson.

TESTING OF CERIUM OXIDE COATED CERMET ANODES IN A LABORATORY CELL

J.S. Gregg, M.S. Frederick, H.L.King, A.J. Vaccaro
ELTECH Research Corporation
625 East Street
Fairport Harbor, Ohio 44077

Abstract

$Cu/NiFe_2O_4/NiO$ cermets were evaluated with and without an in-situ deposited cerium oxyfluoride (CEROX™) coating in 100 hour laboratory Al electrowinning tests. Bath ratio and current density were varied between tests and corrosion was judged by the contamination of the aluminum and cryolite by cermet components (Cu, Fe, and Ni). Higher bath ratios of 1.5 and 1.6 led to less corrosion and thicker CEROX coatings. Lower current densities led to slightly less corrosion but much less oxidation of the Cu cermet substrate. Corrosion of the CEROX coated cermets was 1/7th that of an uncoated cermet. Corrosion of CEROX coated cermets in unsaturated alumina conditions was higher than in saturated tests. The electrical conductivity of the CEROX coating was ~0.2 $\Omega^{-1}cm^{-1}$, resulting in a slight voltage penalty, depending on the thickness of the coating.

Introduction

Inert anodes have been sought to replace carbon anodes in Al electrowinning for many years. The Aluminum Company of America (Alcoa) developed a cermet that was designed to combine the benefits of a metal (good thermal shock resistance and high electrical conductivity) and a ceramic (oxidation resistance) and minimize the shortcomings of each material (1). The material, a $Cu/NiO/NiFe_2O_4$ cermet, performed well in early laboratory testing. After Alcoa discontinued their research program, Battelle Pacific Northwest Laboratories (PNL) continued experimentation with the Cu cermet from 1986 to the present time. After promising laboratory testing of the material, PNL operated a prototype anode for over 100 hours (2,3). The aluminum metal from that test contained over 8% impurities and the anode experienced a 6 mm decrease in diameter. These results were very different from the Alcoa and PNL laboratory results and were not entirely explained. In spite of the prototype anode test results, the Cu cermet remained the best inert anode candidate.

In 1982, it was discovered that a fluorine containing CeO_2 coating could be anodically deposited from a molten cryolite electrolyte when CeO_2 was added to the bath (4). The coatings (known as CEROX™)[a] were found to reduce corrosion of inert anode substrates. In 1986 ELTECH studied the CEROX coating on SnO_2 and Cu cermet substrates (fabricated by PNL) in research supported by the U.S. Department of Energy (DOE) (5). In 8 hour tests, it was demonstrated that the CEROX could be deposited on both substrates and reduced the corrosion of both.

From 1987 through 1992, ELTECH studied the CEROX coating on the leading inert anode candidate, Cu cermets, in Phase II and Phase III programs supported by the U.S. DOE. Some of the results of those tests will be discussed in this paper, but greater detail of the tests is available in the final reports for both projects (6,7). Most of the experiments were operated for 100 hours, with and without a CEROX coating, to determine (1) the optimum bath ratio and current density operation with a CEROX coating on Cu cermets and (2) to define the protection factor afforded by the coating. Most tests were performed under saturated alumina conditions, but several tests were also conducted at 50 to 90% of saturation to determine the affect of lower alumina contents on CEROX deposition and Cu cermet corrosion.

Experimental Methods

Cu cermet anodes were fabricated by ELTECH for the Phase II and III programs. In Phase II, the $NiO/NiFe_2O_4$ powder was fabricated by mixing NiO and Fe_2O_3 together in the 5324 composition of Alcoa (1) and calcining at 900°C. 17 wt% Cu metal was blended with the calcined powder and the anodes were isopressed and sintered at 1350°C for 0.5 h. Densities achieved averaged 5.7 g/cm^3, or about 93 to 94% of theoretical density (TD). A typical microstructure is shown in Figure 1. (All SEM micrographs have been slightly reduced for this publication. Therefore, micron markers are accurate but magnifications are not). During sintering, some of the Cu metal squeezed out onto the surface of the anode and was mechanically removed prior to testing. This resulted in less than 17 wt% Cu in the final anode mixture. At the end of Phase II, two perceived weaknesses of the ELTECH fabricated cermet material were the high porosity (as fabricated) and the continuous Cu metal phase. Therefore,

in Phase III, those aspects in the material were changed in an attempt to achieve a Cu cermet that was similar to the one Alcoa originally tested.

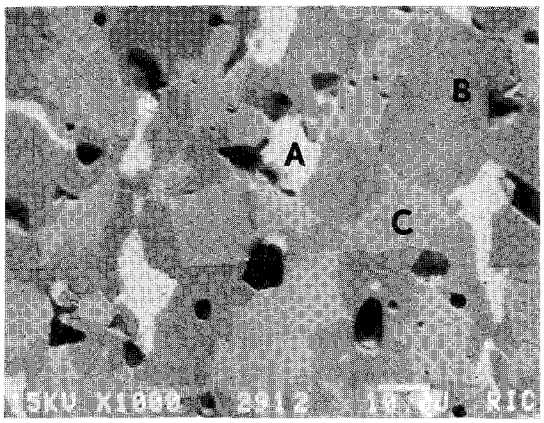

Figure 1: The microstructure of the Cu cermets from the Phase II project consists of Cu (A), $NiFe_2O_4$ (B) and NiO (C), Pores appear as dark holes.

The Phase III cermet was produced from spray dried $NiO/NiFe_2O_4$ powder fabricated by Ceramic Magnetics, Inc. and is of the Alcoa 5324 composition (1). The powder was blended with 17 wt% Cu metal powder, and then isopressed and sintered at 1300°C for 8 hours. Densities of cermets were ~5.99 to 6.1 g/cm^3, 98 to 100% of TD. The microstructure is shown in Figure 2. The Cu grains (A) were 15 to 80 μm in diameter and irregular in shape. The NiO (C), also irregular in shape, was 10 to 35 μm in diameter. The $NiFe_2O_4$ (B) was 10 to 45 μm and rounded. The NiO was actually an (Ni,Fe)O solid solution with ~85 wt% NiO and 15 wt% FeO while the Cu metal was an alloy consisting of ~85 wt% Cu, 11 wt% Ni, and 4 wt% Fe.

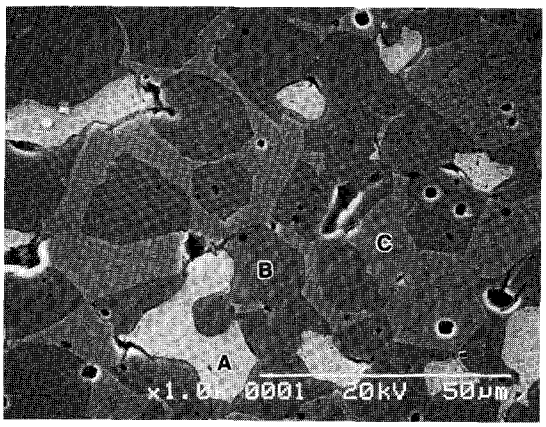

Figure 2: The microstructure of the Phase III Cu cermet is similar to that of Phase II and contains Cu (A), $NiFe_2O_4$ (B) and NiO (C).

The anodes employed during the Phase II program were flat bottomed (0.85 cm radius) while those for the Phase III were rounded (0.77 cm radius) to allow for better release of oxygen bubbles (Figure 3). In addition, an alumina sheath was added in Phase III to prevent any contamination of the bath by cermet components from above the bath. Immersion depth was measured by the electrical contact with the cryolite melt. Immersion in Phase II averaged 3/16" (0.48 cm) while immersion in Phase III was to the top of the rounded bottom, 0.3" (0.77 cm). In Phase II, current density was calculated based on the bottom surface area of the anode. However, some current flow was probably through the sides of the anode. It was estimated that 80% of the current flow was through the bottom of the anode, which resulted in a lower real bottom current density than originally calculated. In Phase III, current density was assumed to be even along the hemispherical tip. Therefore current densities were lowered by 20% to be comparable to the Phase II bottom surface current density.

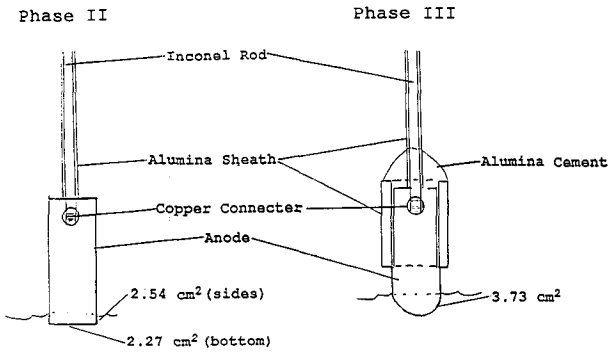

Figure 3: Comparison of Phase II and Phase III anode shape, surface area of immersion region, and anode connections.

The long term test cell is shown in Figure 4. The cathode was the graphite crucible, which was lined with alumina to limit the active area to the bottom of the cell. Aluminum metal (~40 g) was added to the cell prior to testing and, during testing, mixed with the electrolytically produced Al, which accumulated on the bottom of the cell. The appropriate bath mixture was added to the cell and then the cell was heated up to ~970°C. After the bath was molten, the anode was lowered into the melt and electrolysis was begun. Because some of the carbon bottom was exposed to cryolite, Na intercalated into the carbon, causing the bath ratio to decrease. The bath ratio was analyzed periodically throughout the test and additions of NaF or Na_2CO_3 were made to correct it to the desired level. Bath ratio generally ranged from +0.05 above to -0.10 below the target bath ratio. Al_2O_3 and CeF_3 additions were made hourly, assuming current efficiencies of 35 to 75% (depending on the experiment). Bath mixtures consisted of American Fluoride or Washington Mills cryolite, AlF_3 or NaF to achieve the desired bath ratio, 5 wt% CaF_2, 8 wt% Al_2O_3, and 1 wt% CeF_3.

Saturated alumina tests were operated at bath ratios of 1.2 to 1.7 and current densities of 0.5 to 1.9 A/cm^2. The Phase II and Phase III tests conditions are shown in Figure 5. Numbers refer to the experiment numbers in the Phase III tests. Based on the results of the Phase II experiments, Phase III encompassed higher bath ratios at a range of current densities.

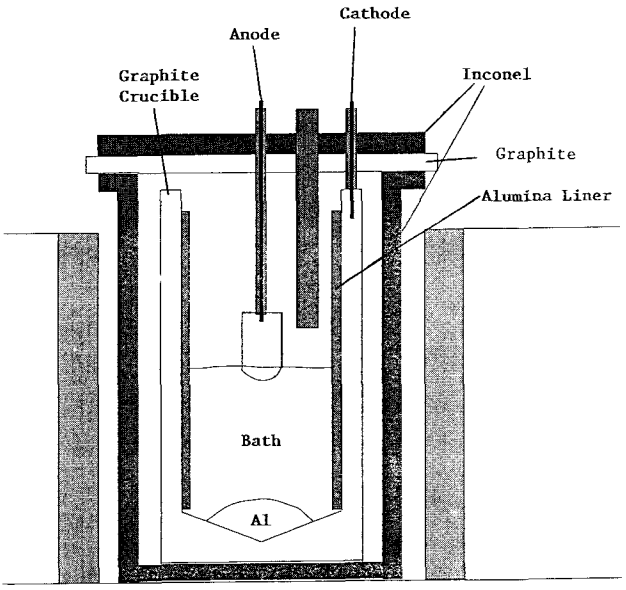

Figure 4: Long-term (100 hour) test cell.

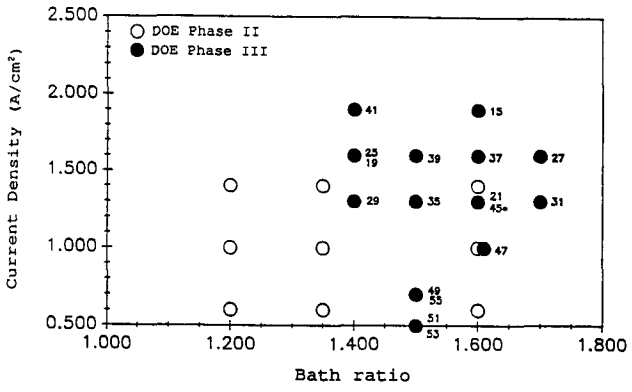

Figure 5: Test conditions for Phase II and Phase II experiments.

Because the long-term test cell had an alumina liner, it was only suitable for tests saturated in alumina. A second test cell was designed for unsaturated alumina tests (Figure 6). The cell was composed of an unlined, nonelectrolyzed graphite crucible. The bottom of the cell was made of frozen cryolite with a small graphite plug within the center to carry the current. The electrical connection to the graphite plug was alumina sheathed Inconel 600. The electrical connection of the Inconel to the graphite was made in the bottom, cooler section of the cell. The bottom cryolite plug and the bottom of the cell were kept cool by placing them below the level of the heating elements in the furnace. In addition, the cryolite plug was composed of pure, high melting point cryolite. Aluminum collected in the center of the frozen cryolite bottom, over the graphite plug. Electrical isolation between the cathode and the graphite crucible was always maintained. The test cell operation was the same as for the long-term saturated test cell, but in addition, Al_2O_3 levels were monitored and additions were made to maintain the desired concentration. Some melting of the top of the solid cryolite occurred, necessitating some bath mixture additions near the beginning of the tests to compensate for the additional molten pure cryolite bath. CeF_3 added at the start of the test was 2 wt% instead of 1 wt% to compensate for the melting of the cryolite bottom.

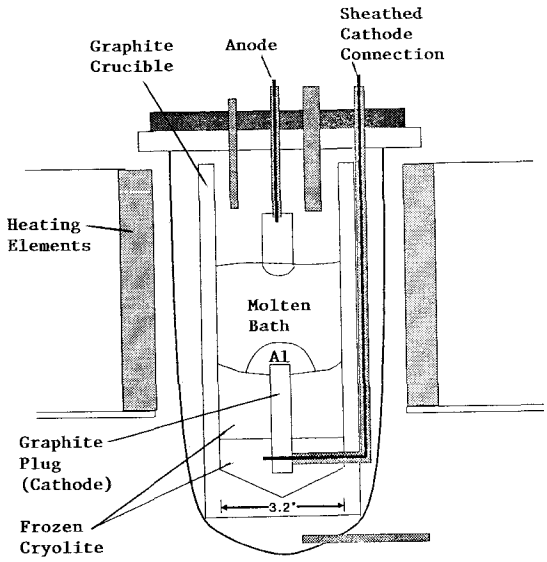

Figure 6: Test cell for unsaturated alumina tests.

CEROX resistance testing was conducted in a small rotating cylinder cell (Figure 7). In this cell the cathode was the graphite liner within an alumina crucible. Tests were only operated for ~5 hours and no aluminum was added to the cell at the start of the test. Therefore, no problem with Al bridging the gap between the anode and cathode was noted. Four experiments with CeF_3 concentrations of 0, 1.8, 3.1, and 4.5 wt% were operated. The anodes were operated for 5 h at 240 mA/cm^2 with a potentiostat to deposit the CEROX coating. After the coating period the current was set to zero and the system equilibrated for 10 to 15 minutes. Then, current pulses 0.1 ms in duration were applied at 5 different amplitudes (30, 90, 150, 210, and 240 mA/cm^2) at 5 rotation rates (0, 500, 1000, 1500, and 2000 rpm). The current pulse and voltage response were recorded on an oscilloscope. Measurements were taken from the anode to the cathode and from the anode to a molybdenum-hook reference electrode (8). No difference was found in resistances calculated from measurements taken with or without the reference.

Results and Discussion

Saturated Alumina Tests

At the end of each test, the cryolite was ground, weighed, and analyzed by ICP for Fe, Ni, Cu, and Ce and the aluminum metal was weighed and analyzed for the same elements. Estimates of current efficiency were made based on the recovered weight of the aluminum. The Fe, Ni, and Cu contamination of the Al and bath were "normalized". Normalization consisted of converting the ICP results to grams of Fe, Ni, and Cu, adding together the bath and metal impurity values, subtracting background corrosion, and

calculating an "industrial" value of Al contamination based on 95% current efficiency.

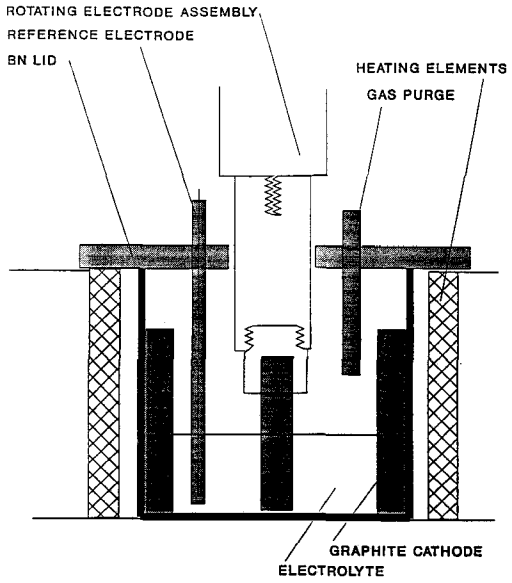

Figure 7: CEROX resistance test cell.

In Phase II, the lowest corrosion achieved (0.04 wt% Fe, 0.05 wt% Ni, 0.06 wt% Cu, 0.15 wt% total impurities) was at a bath ratio of 1.6 and a current density of 1.4 A/cm^2. In addition, the CEROX coating was densest and thickest on that anode (Figure 8). The CEROX coating was ≥1 mm thick on the sides and outer bottom edges, while the coating was thinner on the flat bottom of the anode, where it appeared that oxygen had collected. In contrast to Figure 8, Figure 9 shows the thin and discontinuous CEROX coating (≤200 μm) developed at a bath ratio of 1.2 and current density of 1.0 A/cm^2. Phase II demonstrated that higher bath ratio led to thicker and denser CEROX coatings while low bath ratio led to thinner coatings.

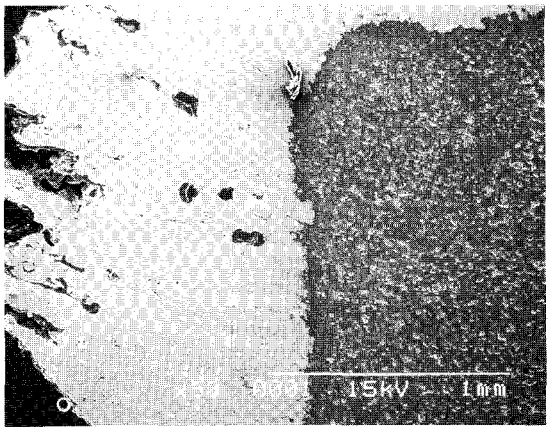

Figure 8: The CEROX coating from the Phase II experiment conducted at a bath ratio of 1.6 and a current density of 1.4 A/cm^2 is dense and ~ 1 mm thick.

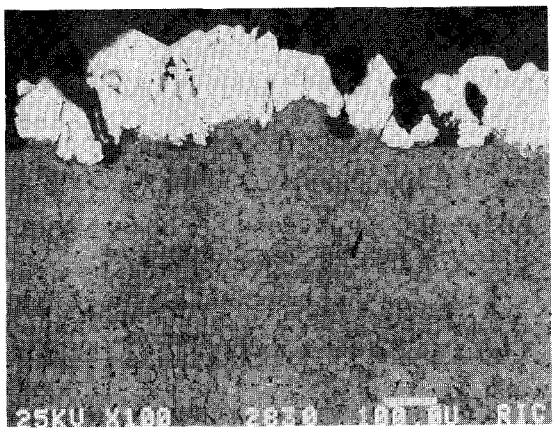

Figure 9: The CEROX coating from the Phase II experiment conducted at a bath ratio of 1.35 and current density of 1 A/cm^2 is ≤ 200μm thick and discontinuous.

A Ce-free Cu cermet was operated at a bath ratio of 1.35 and current density of 1.0 A/cm^2 and corrosion compared to an anode operated under the same conditions with Ce. The corrosion for the two anodes was 6.27 wt% Fe, 0.75 wt% Ni, 0.63 wt% Cu, and 7.65 wt% total corrosion for the uncoated anode compared to 0.18 wt% Fe, 0.08 wt% Ni, 0.75 wt% Cu, and 1.01 wt% total corrosion for the CEROX coated anode. This shows that the CEROX coating reduced total corrosion to 1/7 that of the uncoated anode.

Since the best coatings and least corrosion occurred at a bath ratio of 1.6 and a current density of 1.4 A/cm^2 in Phase II, Phase III test conditions were chosen to bracket those conditions. Normalized corrosion for bath ratios from 1.4 to 1.7 at current densities of 1.3 and 1.6 A/cm^2 is shown in Figures 10 and 11. At 1.3 A/cm^2, there was a minimum in corrosion at a BR of 1.5 to 1.6. At 1.6 A/cm^2, no trend was evident and total corrosion appeared to be higher at all bath ratios.

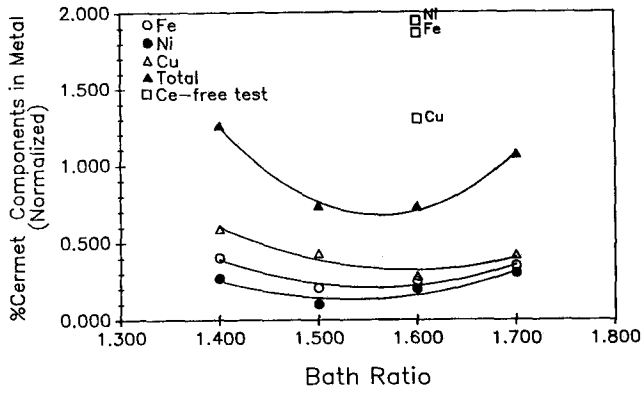

Figure 10: Corrosion as a function of bath ratio at 1.3 A/cm^2.

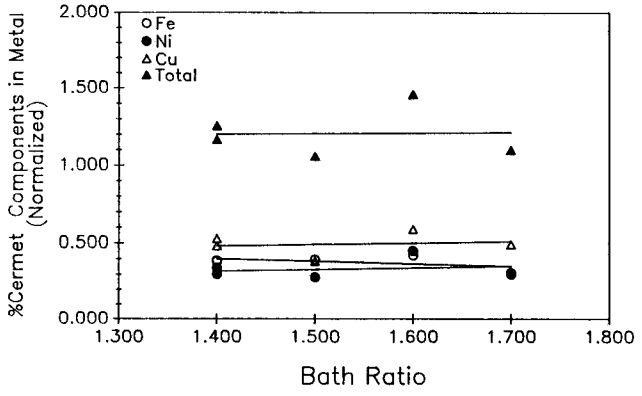

Figure 11: Corrosion as a function of bath ratio at a current density of 1.6 A/cm^2.

Comparison of corrosion as a function of current density is shown in Figures 12 and 13 for bath ratios of 1.5 and 1.6. At both bath ratios, there is a slight decrease in corrosion with decreasing current density. An uncoated Cu cermet, operated at a bath ratio of 1.6 and current density of 1.3 A/cm^2, had a corrosion of 1.87 wt% Fe, 1.95 wt% Ni, 1.30 wt% Cu, and 5.11 wt% total corrosion. An anode operated at the same conditions with a CEROX coating had a corrosion of 0.25 wt% Fe, 0.20 wt% Ni, 0.28 wt% Cu, and 0.732 wt% total impurities. As in Phase II, the CEROX coating reduced total corrosion to 1/7 that of the uncoated Cu cermet anode.

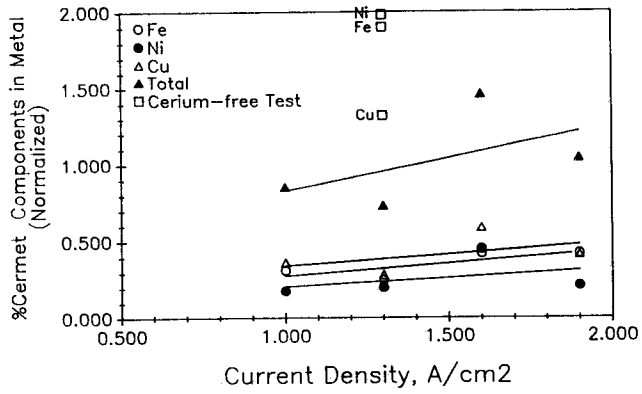

Figure 12: Corrosion as a function of current density at a bath ratio of 1.5.

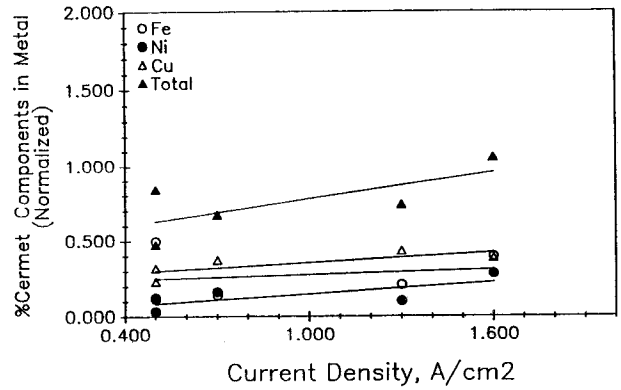

Figure 13: Corrosion as a function of current density at a bath ratio of 1.6.

As in Phase II, in Phase III CEROX coatings were thickest and densest at higher bath ratios. Macroscopic photos demonstrate the difference between the coatings developed at a bath ratio of 1.4 and at a bath ratio of 1.6. At a bath ratio of 1.4, the CEROX coating was irregular in thickness and discontinuous. In addition, the interface between the substrate and the CEROX coating was irregular, indicating dissolution of the cermet (Figure 14). A CEROX coating formed at a bath ratio of 1.6 (Figure 15) is dense and more regular in thickness. The interface between the Cu cermet substrate and the coating is smoother, indicating less corrosion. An SEM micrograph (Figure 16) of the CEROX coating formed at a bath ratio of 1.6 shows how dense and continuous the coating is, although some closed pores are present near the substrate interface.

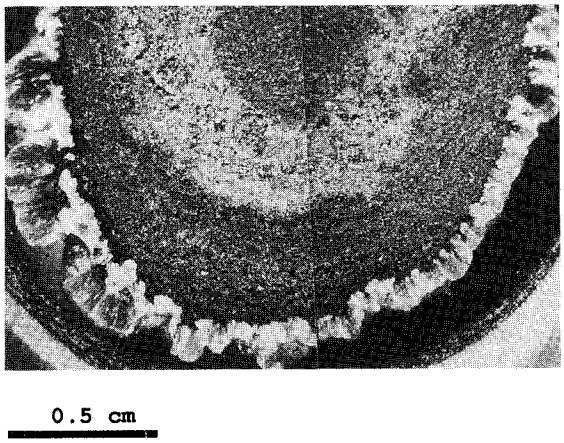

Figure 14: Irregular CEROX coating developed at a bath ratio of 1.4.

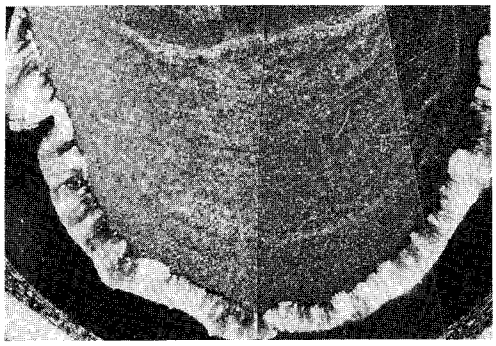

Figure 15: Dense, continuous CEROX coating developed at a bath ratio of 1.6.

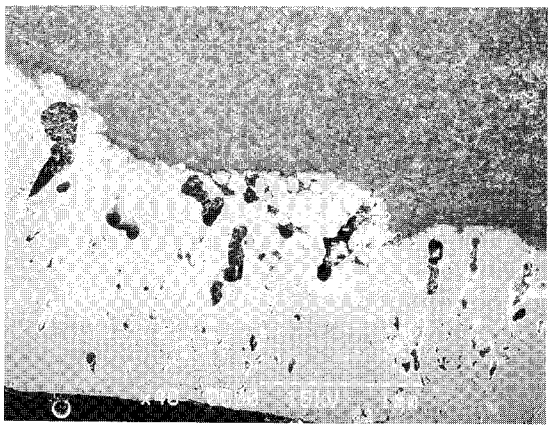

Figure 16: The CEROX coating (light colored), formed at a bath ratio of 1.6 is thick and dense with some closed pores (black) near the Cu cermet substrate (top of photo).

A macroscopic photo of the uncoated Cu cermet anode, operated at the same electrolysis conditions as the anode in Figure 15 (bath ratio of 1.6, current density of 1.3 A/cm^2), is shown in Figure 17. The tapering of the anode and loss of material (all anodes were originally 0.77 cm radius) demonstrate the degree of corrosion that occurred during the 100 hour test. In comparison, the anode in Figure 15 showed no macroscopic tapering or loss of material.

Figure 17: An uncoated Cu cermet anode, tested at the same conditions as the anode in Figure 15 (100 hours, 1.6 bath ratio, 1.3 A/cm^2 current density). (White on the tip is frozen cryolite).

Figure 18 is a SEM micrograph of an anode with relatively low corrosion (0.74 wt% total corrosion) but with a slightly discontinuous CEROX coating. It is evident that the CEROX coating protects the substrate from corrosion where the thick coating (~1 mm) is present and that the substrate is more corroded (Location A) where the thick coating is absent. In addition, in the corroded areas, a thin CEROX coating has redeposited on the corroded substrate.

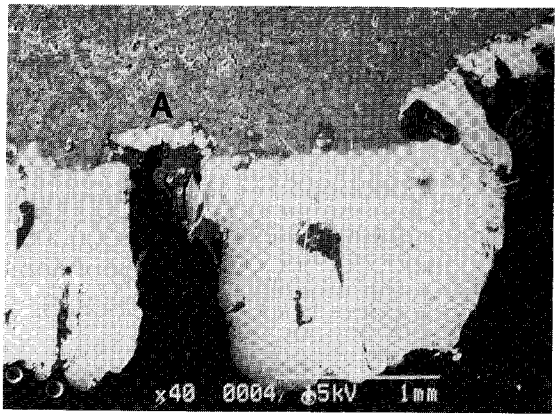

Figure 18: An anode operated at a bath ratio of 1.5 and current density of 1.3 A/cm^2 had low corrosion but does exhibit more corroded regions where the CEROX coating is thin (location A). The CEROX coating appears white in the SEM micrograph and the substrate is gray.

The two lowest corrosion test conditions in Phase III were at a bath ratio of 1.5 and current densities of 0.5 and 0.7 A/cm^2. In these tests corrosion was 0.123 wt% Fe, 0.032 wt% Ni, 0.317 wt% Cu, and 0.471 wt% total corrosion at 0.5 A/cm^2 and 0.138 wt% Fe, 0.162 wt% Ni, 0.370 wt% Cu, and 0.670 wt% total corrosion at 0.7 A/cm^2. These values are not as low as the best experiment from Phase II but the CEROX protection factor from Phase II and III is the same and the trend toward lower corrosion and denser CEROX coatings at a bath ratio of 1.5 to 1.6 is consistent.

Ce partitioning between the metal and the bath was measured at the end of each test (Figure 19 and 20). The Ce levels in the Al metal ranged from ~1.5 to ~2.4 wt% while those in the bath ranged form 0.15 to 0.25 wt%. The Ce partition coefficient (Ce_{metal}/Ce_{bath}) ranged from ~6 to ~12, and appeared to increase slightly with increasing bath ratio (Figure 21).

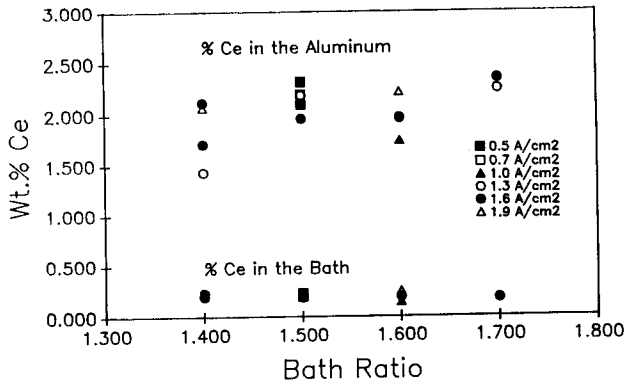

Figure 19: Ce levels in the aluminum and the cryolite bath.

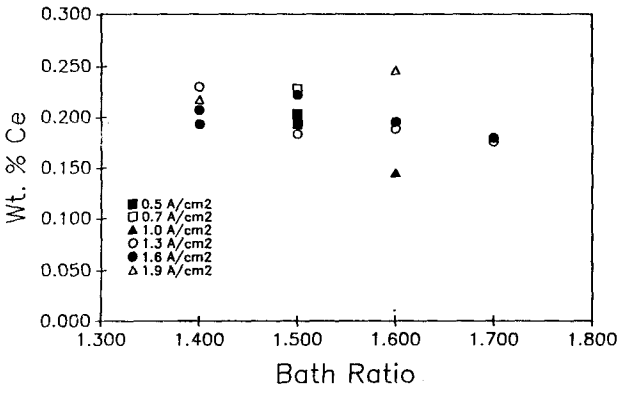

Figure 20: Ce concentrations in the cryolite baths.

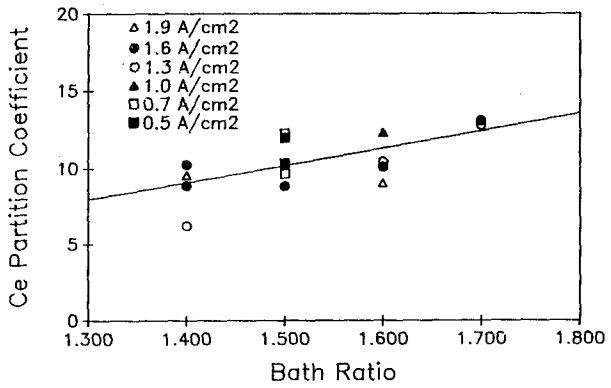

Figure 21: Ce partition coefficient as a function of bath ratio.

Unsaturated Alumina Tests

Unsaturated tests with 6 wt% alumina (~75% of saturation) were operated at the same test conditions that produced the lowest corrosion in the saturated alumina tests. Tests were performed at a bath ratio of 1.5 and current density of 0.5 and 0.7 A/cm^2, and at a bath ratio of 1.6 and current density of 0.7 A/cm^2. In addition, at a bath ratio of 1.5 and current density of 0.5 A/cm^2, tests were operated with 4 and 7.2% alumina (~50 and 90% of saturation). Bath ratio control was similar to that for the saturated tests (-0.1 to +0.05) while alumina concentration was normally ~$\pm$1%. The test at 4% alumina operated for a short time at higher alumina concentrations and the test at 7.2% operated for a short time at 4% alumina. There was little difference in the corrosion between all the tests operated at 6 wt% alumina. However, as shown in Figure 22, at a bath ratio of 1.5 and current density of 0.5 A/cm^2, corrosion increased with decreasing alumina concentration. The saturated test at the same test conditions is shown in Figure 22 for comparison.

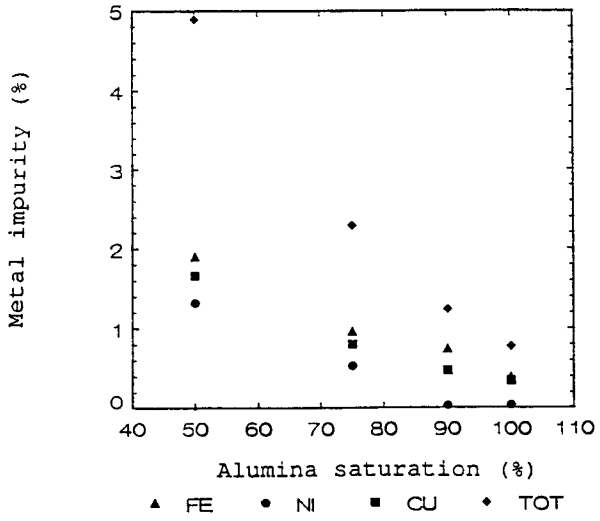

Figure 22: Fe, Ni, Cu and total corrosion in tests with 50 to 100% of alumina saturation.

Since more Ce was added to the unsaturated tests to compensate for some of the melting of the cryolite bottom of the cell, the Ce concentrations in the bath (0.18 to 0.7 wt%) and metal (2.3 to 3.7 wt%) were generally higher than in the saturated tests but partition coefficient was similar, ranging from 5 to 17. The higher levels of Ce in the bath led to thicker CEROX coatings (1 to 5 mm) on the anodes (Figure 23). In these coatings the inner 1 to 2 mm was dense while the outer region was porous.

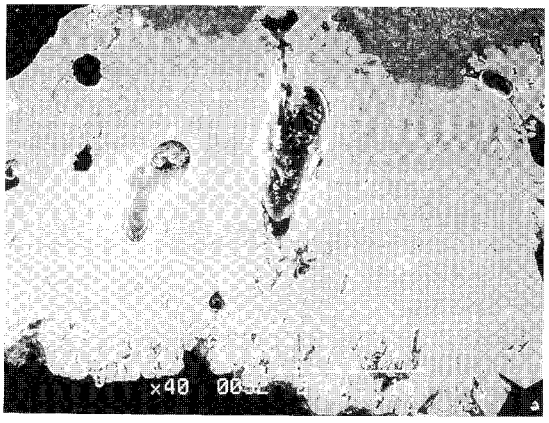

Figure 23: CEROX coating formed at a bath ratio of 1.5, current density of 0.5 A/cm.^{2}, and with 6 wt.% alumina in the bath.

Cu Cermet

The Cu cermet substrates in both the saturated and unsaturated alumina tests underwent microstructural changes during the testing. Next to the CEROX coating (A), there was a ~200 to 1100 μm thick Cu depleted layer (B) that consisted of NiO and $NiFe_2O_4$ (Figure 24). Next, an oxidized region with Cu oxide (probably Cu_2O), NiO, and $NiFe_2O_4$ was 0.5 to >20 mm thick (C in Figure 24). In the interior of the anode, Cu metal was still present with NiO and $NiFe_2O_4$. The boundary

between the Cu metal region and the oxidized region was always distinct (Figure 25). In anodes that had extensive oxidation, alternating Cu oxide-rich and Cu oxide-poor bands were developed within the oxidized region (Figure 26). In addition, porosity was increased in the oxidized areas relative to the untested cermet, and porosity was even higher in the Cu oxide-poor bands.

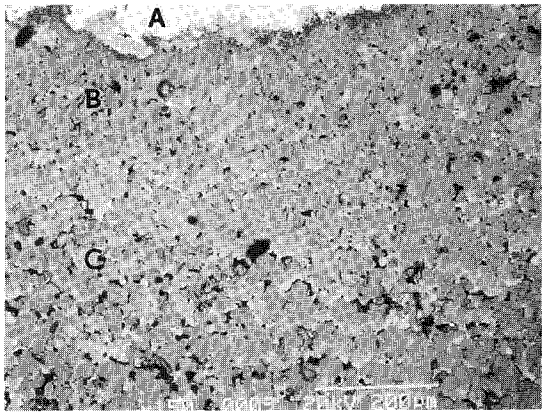

Figure 24: Next to the CEROX coating (A), within the substrate, there is a Cu depleted region (B) and then a Cu oxidized region (C). This is typical of all tested Cu cermets.

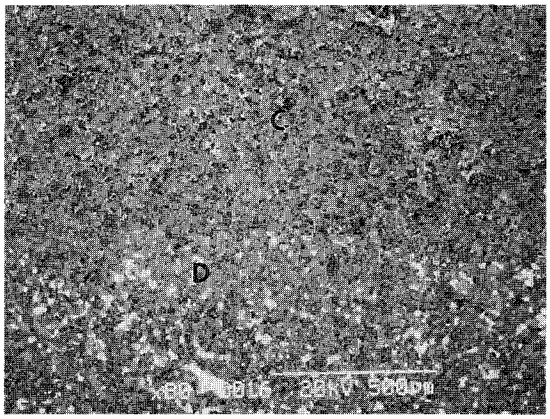

Figure 25: The boundary between the Cu oxidized region (C) and Cu metal region (D) is sharp in all samples. Both regions also contain NiO and $NiFe_2O_4$.

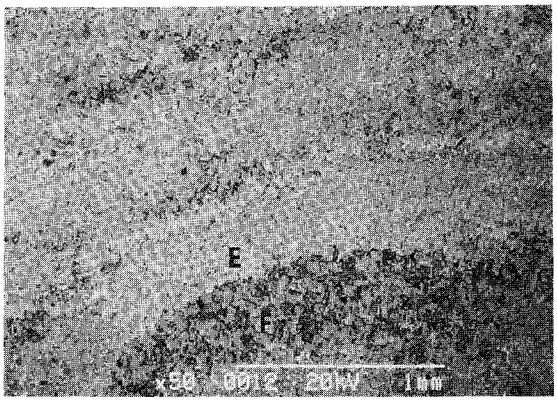

Figure 26: Alternating Cu oxide-rich (E) and Cu oxide-poor (F) bands in an anode that had undergone extensive oxidation. The CuO appears white in the SEM micrograph.

The composition of the NiO, Cu, Cu oxide, and $NiFe_2O_4$ phases in the untested and tested material is shown in Table I. In the tested anodes, the Cu metal and Cu oxide were enriched in Cu and depleted in Ni relative to the Cu metal in the untested material. The NiO in the tested samples was enriched in Cu and Ni and depleted in Fe compared to the untested material. In the untested cermet, the $NiFe_2O_4$ was slightly Fe rich compared to the stoichiometric ferrite (~32 wt% NiO, ~68 wt% Fe_2O_3). The composition of the ferrite appeared to become more stoichiometric in the tested anode, particularly in the oxidized region.

Table I Average Phase Compositions

	Phase Composition (wt.%)		
Untested Anode	Cu	NiO	$NiFe_2O_4$
Center	85.2 Cu 11.1 Ni 3.7 Fe	84.1 NiO 14.9 FeO 1.0 CuO	72.8 Fe_2O_3 26.4 NiO 0.8 CuO
Tested Anode	CuO	NiO	$NiFe_2O_4$
Center area with metallic Cu	94.0 Cu 3.0 Fe 3.0 Ni	90.8 NiO 7.9 FeO 1.3 CuO	70.0 Fe_2O_3 29.0 NiO 1.0 CuO
Oxidized area	96.5 CuO 2.8 FeO 1.6 NiO	87.3 NiO 9.6 FeO 3.1 CuO	67.4 Fe_2O_3 31.6 NiO 1.0 CuO

The amount of oxidation within the anodes was related to the current density. In both Phase II and Phase III, after 100 hours of testing, oxidation thickness was 1.0 to 1.3 mm at 0.5 A/cm^2, 2.0 mm at 0.7 A/cm^2, and 3.5 to 4.5 mm at 1.0 A/cm^2. At higher current densities, oxidized thicknesses were greater than the radius of the anode. In anodes that were extensively oxidized, cell voltage increased during testing. Typically, cell

voltage was 3 to 3.5 V throughout the test. However, on the most highly oxidized anodes, cell voltage rose to $\geq$ 6 V by the end of the 100 hour test.

Electrical Conductivity of CEROX

To determine the electrical conductivity of the CEROX coating, rotating electrode experiments were performed. A model was constructed assuming the system behaved linearly [Figure 27 (a)]. The model accounted for the resistances of the electrolyte (R_e), coating (R_c), and the two interfaces (R_i:anode-coating interface, R_{ct}: coating-electrolyte interface), the possible capacitances of the coating (C_c) and the two interfaces (C_i: anode-coating interface, C_{dl}: coating-electrolyte interface). The cermet was assumed to have negligible resistance. An impedance was also added to account for mass transfer effects (W_{mt}).

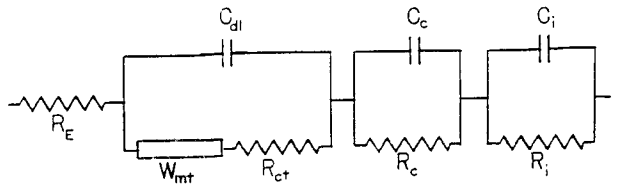

Figure 27 (a): Electric circuit model of the system.

R_{ct} and W_{mt} are the charge transfer resistance and the mass transfer impedance of the reaction occurring at the coating surface. At high temperatures, R_{ct} is often reduced because kinetics are generally fast. W_{mt} is also less important at high temperatures because the diffusion coefficient of the reactants increases with temperature. If R_{ct} and W_{mt} were negligible at the high temperature of this system, the modelling circuit would reduce to that shown in Figure 27 (b). The electrolyte resistance was determined from the electrolyte conductivity, which was measured. The remaining resistances were due only to the coating.

Little change in resistance was detected for increased current density, and therefore the system was considered to behave linearly. Changes in the rotation rate of the anode had little effect on the measured resistance, thus mass transfer resistance (W_{mt}) was considered to be negligible. No charging was seen in the voltage responses to the current pulses, indicating that either R_{ct} or C_{dl} was very small. Therefore, the circuit for the Cu cermet system reduced to the simplified model shown in Figure 27 (b). The resistance of the solution and experimental apparatus were defined in the 0% CeF_3 experiment, allowing for calculation of the resistance of the CEROX coating in the experiments conducted with 1.8, 3.1, and 4.5 wt% CeF_3. Figure 28 shows the calculated conductivity of the CEROX coating. Error bars indicate the ranges of uncertainty in the original resistance measurement from the oscilloscope. Conductivity averaged ~0.20 ±0.05 $\Omega^{-1}cm^{-1}$.

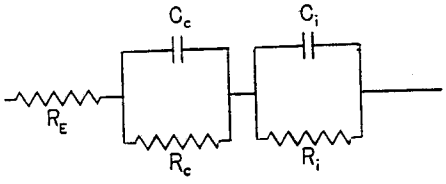

Figure 27 (b): Simplified circuit model.

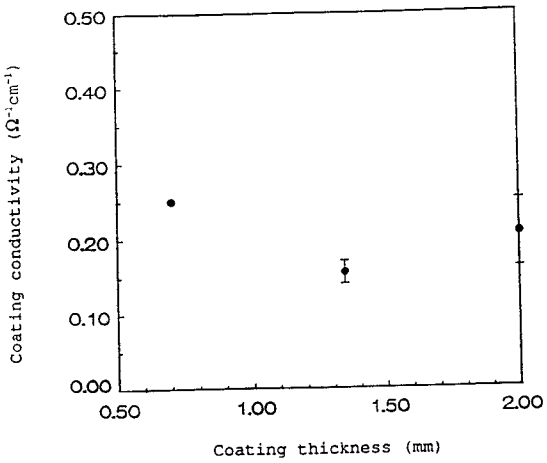

Figure 28: Electrical conductivity of the CEROX coating.

The added energy cost associated with the coating resistance was calculated. If anodes are operated at 0.7 A/cm^2, and the process has a current efficiency of 90%, a 1 mm thick coating having a conductivity of 0.2 $\Omega^{-1}cm^{-1}$, would add $26.21 to the cost of producing 1 ton of Al. This calculation assumes an energy cost of 2.5 cents/kW·h. Cost savings due to the use of CEROX coated inert anodes instead of carbon anodes may offset this cost.

Conclusions

The Phase II and Phase III projects were successful in defining the optimum conditions for CEROX coatings and protection on the Cu cermet substrate, for demonstrating the increase in corrosion in baths unsaturated with alumina, for defining the CEROX protection factor of the Cu cermet, and for accurately defining the electrical conductivity of the CEROX coating.

Specifically the conclusions are

- The CEROX coating is densest, most continuous, and minimizes corrosion of a Cu cermet at a BR of 1.5 to 1.6.
- A CEROX coating reduces the corrosion of a Ni ferrite/Cu cermet to 1/7 that of an uncoated cermet.
- In unsaturated alumina baths, CEROX coatings could be formed on the anodes but cermet corrosion increased with decreasing alumina concentration. Corrosion was still less than in saturated tests with an uncoated Cu cermet.
- Oxidation and Cu depletion occurred in the tested Cu cermet and was associated with increased porosity and changes in the phase composition. Oxidation thickness was greater at higher current density. In the anodes that underwent extensive oxidation, cell voltage increased as the test progressed.
- The conductivity of the CEROX coating is ~0.2 $\Omega^{-1}cm^{-1}$ which translates into an increased energy cost of ~$25/ton of aluminum based on a price of 2.5 cents/kW·h, 90% CE, and operation with a 1 mm thick coating at 0.7 A/cm^2.

Acknowledgements

This material was prepared with the support of the U.S. Department of Energy (DOE Cooperative Agreement No. DE-FC07-90ID12949). However, any opinions, findings, conclusions, or recommendations expressed herein are those of the authors and do not necessarily reflect the view of DOE.

References

1. J.D. Weyand et al., "Inert Anodes for Aluminum Smelting," (Report DOE/CS/40158-20, Alcoa Final Report to U.S> DOE, February 1986).

2. D.M. Strachan et al., "Inert Electrodes Program Fiscal Year 1988 Annual Report," (Report PNL-7106/UC-313, Battelle Pacific Northwest Laboratories, October 1989).

3. D.M. Strachan et al., "Results from Electrolysis Testing of a Prototype Inert Anode," (Report PNL-7345/UC-313, Battelle Pacific Northwest Laboratories, May 1990).

4. J.J. Duruz et al., U.S. Patent 4,614,569 (Sep. 30, 1986), assigned to MOLTECH Invent S.A.

5. J.K. Walker, "Cerium Oxide Coated Anodes for Aluminum Electrowinning," (Report DE/ID/12655-1, Final Report by ELTECH Research Corporation to U.S. DOE, February 1986).

6. H.L. King, "Long-Term Testing of In-situ Cerium Oxide-Coated Anodes for Aluminum Electrowinning,: (Report DE/ID/12655-2, Final Report by ELTECH Research Corporation to U.S. DOE, October 1989).

7. J.S. Gregg and M.S. Frederick, "Evaluation of Cerium Oxide Coated Cu Cermets as Inert Anodes for Aluminum Electrowinning," (Report DE/ID/12949, Final Report by ELTECH Research Corporation to U.S. DOE, March 1992).

8. J.W. Burgman, J.A. Leistra, and P.J. Sides, "Aluminum/Cryolite Reference Electrodes for Use in Cryolite-Based Melts," J. Electrochem. Soc., 133 (3) (1986), 496-500.